ELSEVIER

Journal of Alloys and Compounds 434–435 (2007) 311–314

Journal of ALLOYS AND COMPOUNDS

www.elsevier.com/locate/jallcom

Strain-induced microstructural evolution and work softening behavior of Zn–15% Al alloy

Joong-Hwan Jun *, Ki-Duk Seong, Jeong-Min Kim, Ki-Tae Kim, Woon-Jae Jung

Light Materials Team, Advanced Materials R&D Center, Korea Institute of Industrial Technology, 994-32 Dongchun-dong, Yeonsu-gu, Incheon 406-130, South Korea

Available online 2 October 2006

Abstract

Strain-induced microstructural evolution of a Zn–15% Al alloy was studied in order to elucidate the reason for its work softening behavior. Fully annealed microstructure of the Zn–15% Al alloy is distinctively characterized by primary η grains and (η + α) lamellar colonies, where η and α are Zn-rich HCP and Al-rich FCC phases, respectively. Hardness and yield strength decreased continuously with an increase in cold rolling up to 80%, exhibiting work softening behavior. During cold rolling, the (η + α) colonies with interlamellar spacing of ∼100 nm change into equiaxed η and α grains with sizes of ∼500 to ∼800 nm by dynamic recrystallization, whereas primary η grains are only elongated along the rolling direction without any evidence of recrystallization. A linear relationship between volume fraction of recrystallized (η + α) grains and the strength is established. The compositional analyses on primary η grains demonstrate that dissolved Al solutes inside η grains precipitate during cold rolling.

Keywords: Work softening; Zn–15% Al alloy; Dynamic recrystallization; η grains; (η + α) colonies

1. Introduction

Thermally sprayed coating of Zn or Zn alloys currently forms one of predominant groups for corrosion protection of steel and concrete [1]. Surface protection is realized by forming a coating of Zn or Zn alloys in combination with a paint, and the coating is able to form protective layers which can work as sacrificial anode. The most commercially spraying Zn alloys are of binary Zn–Al [1]. Addition of Al to Zn improves the corrosion resistance of coatings dramatically, showing a maximum of corrosion protection at 15% of Al content. Generally, the coating materials are produced as wires and should have optimum tensile strength.

Recently, Yamamoto et al. [2,3] reported that hypo-eutectic Zn–(5–18%) Al alloys and eutectic Zn–22% Al alloy exhibit work softening behavior. Based on changes in electrical resistivity and lattice parameter with respect to degree of cold rolling, they suggested that work softening of Zn-rich Zn–Al alloys is attributable to the recovery and dynamic recrystallization at room temperature, which arises from a decrease in recrystallization temperature in response to the precipitation of dissolved Al solutes from η (Zn-rich HCP phase) grains [3]. However, the reason for work softening of the Zn-rich Zn–Al alloy is still unclear for lack of sufficient micrographical evidence. This study aims to clarify the reasons for work softening behavior of Zn-rich Zn–Al alloys by a systematic investigation on the microstructural evolution with respect to degree of cold rolling for a Zn–15% Al alloy.

2. Experimental

Zn–15% Al alloy (in weight) was prepared by melting 99.995% Zn and 99.99% Al under a protective atmosphere and casting into metallic mould. The ingot was homogenized by keeping at 350 °C for 12 h and hot-rolled into sheets with different thicknesses. All sheets were annealed at 350 °C for 2 h followed by air cooling and cold-rolled at room temperature in a wide range of 0–80% reduction in thickness. The final thickness of the sheets was 2 mm. From these sheets, specimens for tensile tests, X-ray diffraction (XRD) analyses, hardness measurements and microstructural observations were prepared by machining. The chemical composition of the experimental alloy is listed in Table 1. Room-temperature tensile tests were carried out with Instron-type machine with ASTM subsize (gauge length: 25 mm) specimens under initial strain rate of $6.7 \times 10^{-4}\ s^{-1}$ and hardness was measured using a microvickers hardness tester (Matsuzawa MXT-α) with a load of 100 gf. After etching with a 50 g CrO_3 + 4 g Na_2SO_4 + 1000 mL H_2O solution, the microstructures were examined by optical microscope (Olympus CK-40M) and scanning electron microscope (EFI Sirion FESEM) equipped with energy dispersive X-ray spectrometer (EDS). The volume fractions of recrystallized grains were determined in an Image Pro software and phase constituents of the alloy were identified by XRD with Cu Kα radiation.

* Corresponding author. Tel.: +82 32 8500 425; fax: +82 32 8500 410.
E-mail address: jhjun@kitech.re.kr (J.-H. Jun).

0925-8388/$ – see front matter © 2006 Elsevier B.V. All rights reserved.
doi:10.1016/j.jallcom.2006.08.189

Table 1
Chemical composition of experimental alloy

Alloy	Chemical composition (wt.%)			
	Al	Fe	Cu	Zn
Zn–15% Al	15.5	0.022	0.005	Bal.

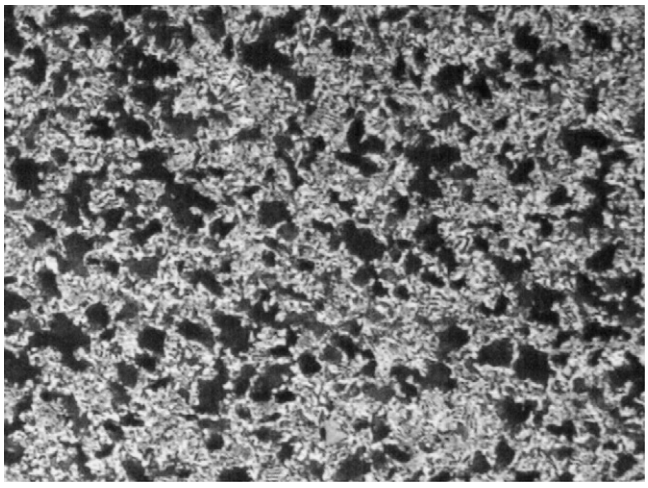

Fig. 1. Optical microstructure of Zn–15% Al alloy in fully annealed state (before cold rolling).

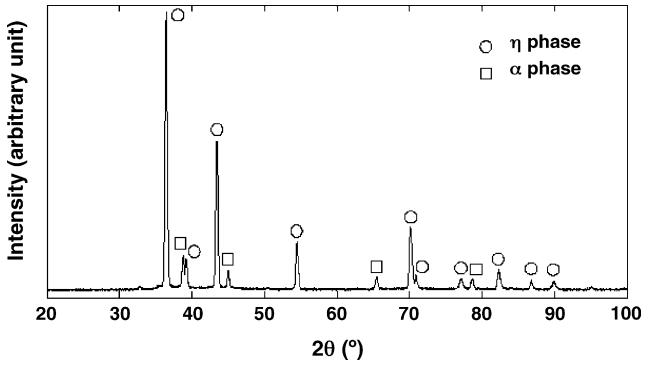

Fig. 2. XRD pattern of Zn–15% Al alloy in fully annealed state.

3. Results and discussion

Fig. 1 shows the optical micrograph of the Zn–15% Al alloy in fully annealed state. The microstructure is characterized by primary η grains (marked "A") and (η + α) lamellar colonies (marked "B"), where η and α are Zn-rich HCP and Al-rich FCC phases, respectively. The XRD pattern of Zn–15% Al alloy before cold rolling is given in Fig. 2. As can be expected from Zn–Al phase diagram [4], only peaks corresponding to η and α phases are seen, indicating no other phases in the microstructure. Fig. 3 represents the changes in Vickers hardness and yield strength of Zn–15% Al with reduction in thickness. Hardness and yield strength decrease continuously with an increase in cold rolling degree, showing work softening behavior.

Fig. 4 shows scanning electron microstructure of Zn–15% Al alloy subjected to 20% cold rolling. It is noticeable that during cold rolling, primary η grains are elongated along the

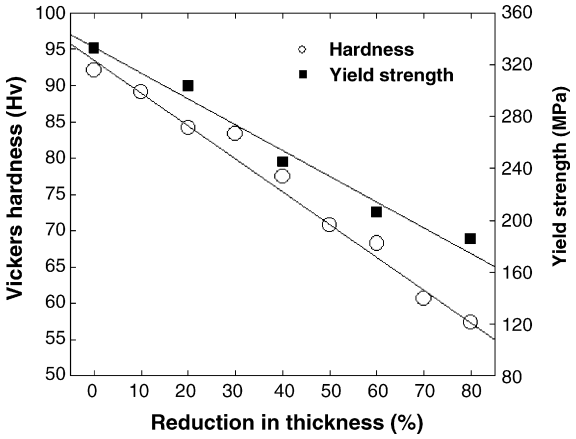

Fig. 3. Changes in Vickers hardness and yield strength with reduction in thickness for Zn–15% Al alloy.

rolling direction, and that nano-sized grains with equiaxed morphology appear inside (η + α) lamellar colonies and near the interfaces between the lamellar colonies and η grains (marked by arrows). The newly observed equiaxed grains may well be η and α phases and generated from (η + α) lamellar colonies by dynamic recrystallization during cold rolling. Scanning electron microstructures of the Zn–15% Al alloy after 40 and 60% cold rolling are given in Figs. 5 and 6, respectively. With the increase in cold rolling, the volume fraction of recrystallized grains is seen to increase. It is noteworthy that the recrystallized grains are not found in primary η grains, indicating an occurrence of dynamic recrystallization only in (η + α) lamellar regions during cold rolling. After 80% cold rolling, most (η + α) lamellar colonies are recrystallized into equiaxed η and α grains with sizes of ∼500 to ∼800 nm as shown in Fig. 7, whereas primary η grains still remain without any evidence of dynamic recrystallization.

The volume fractions of primary η grains (η + α) lamellar colonies and recrystallized η and α grains are plotted as a function of reduction in thickness in Fig. 8. The volume fraction of recrystallized η and α grains increases up to ∼60% after 80% cold rolling, while the volume fraction of (η + α) lamellar colonies decreases from ∼70% (before cold rolling)

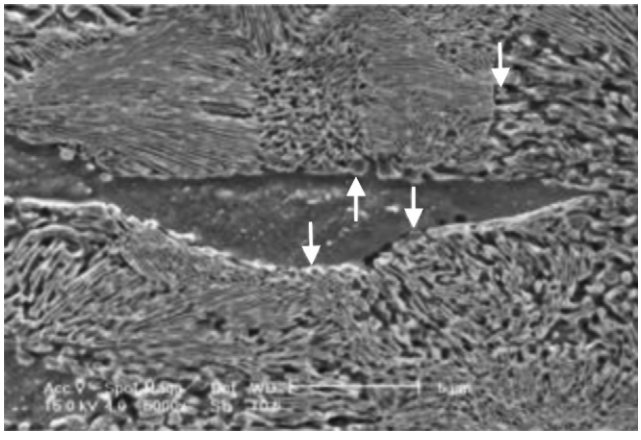

Fig. 4. Scanning electron microstructure of Zn–15% Al alloy subjected to 20% cold rolling (×5000).

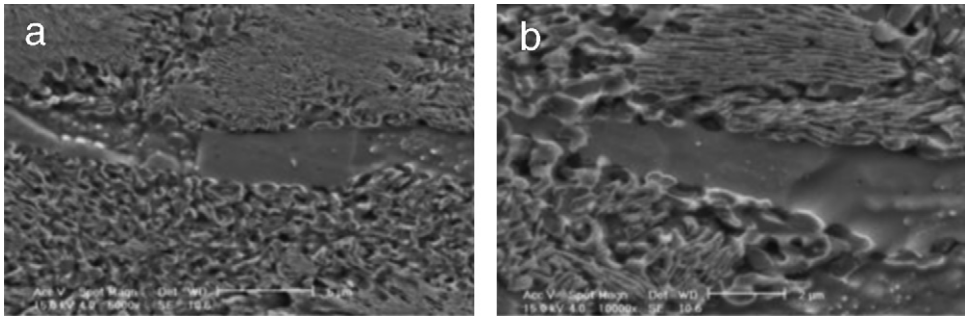

Fig. 5. Scanning electron microstructures of Zn–15% Al alloy subjected to 40% cold rolling: (a) ×5000 and (b) ×10,000.

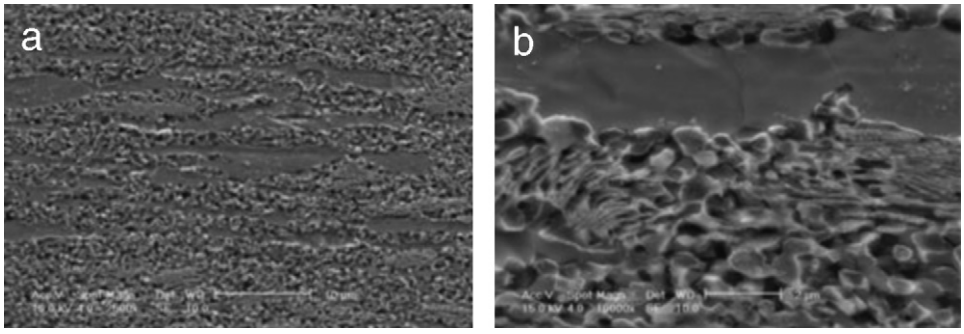

Fig. 6. Scanning electron microstructures of Zn–15% Al alloy subjected to 60% cold rolling: (a) ×2500 and (b) ×10,000.

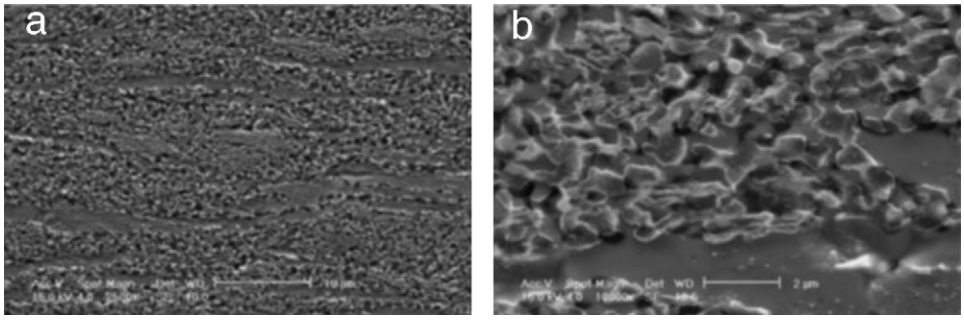

Fig. 7. Scanning electron microstructures of Zn–15% Al alloy subjected to 80% cold rolling: (a) ×2500 and (b) ×10,000.

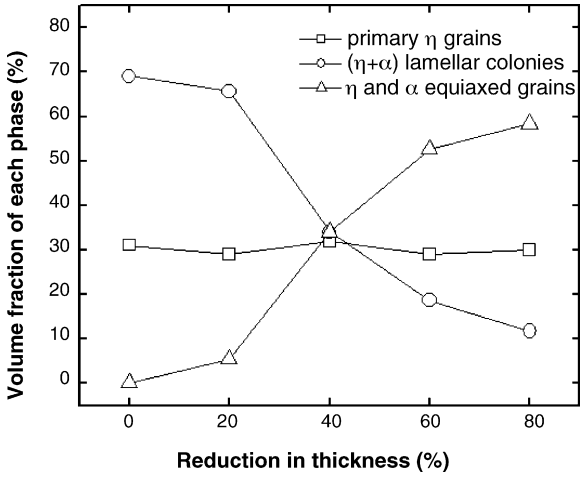

Fig. 8. Changes in volume fraction of primary η grains, (η + α) lamellar colonies and recrystallized η and α equiaxed grains with reduction in thickness for Zn–15% Al alloy.

to ∼10% (after 80% cold rolling). Taking the microstructural evolution in Figs. 4–7 into account, the reasons for work softening behavior of the Zn–15% Al alloy can be explained as follows:

(i) *Structural softness due to morphological change of (η + α) phases from fine lamellar structure to coarse equiaxed grains*. According to Hall–Petch equation [5,6], the strength of microstructure with lamellar or equiaxed morphology is inversely proportional to grain size or interlamellar spacing. The apparent interlamellar spacing having the lowest value (nearly same to true interlamellar spacing) determined by image analysis is ∼100 nm for the (η + α) colonies before cold rolling, which is much smaller than grain sizes of ∼500 to ∼800 nm for the recrystallized η and α phases. Therefore, morphological change of (η + α) lamellar colonies to equiaxed η and α grains may well give rise to the structural softness.

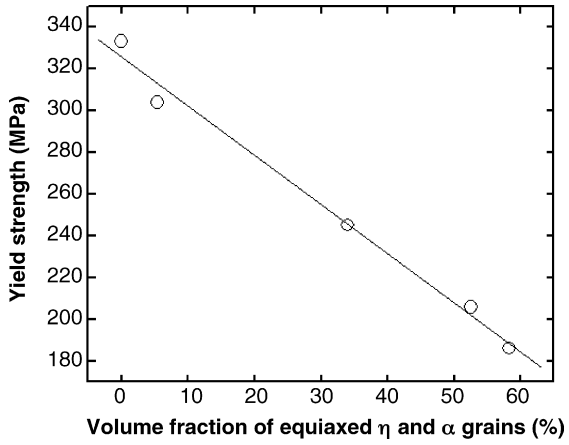

Fig. 9. Change in yield strength with volume fraction of equiaxed η and α grains for Zn–15% Al alloy.

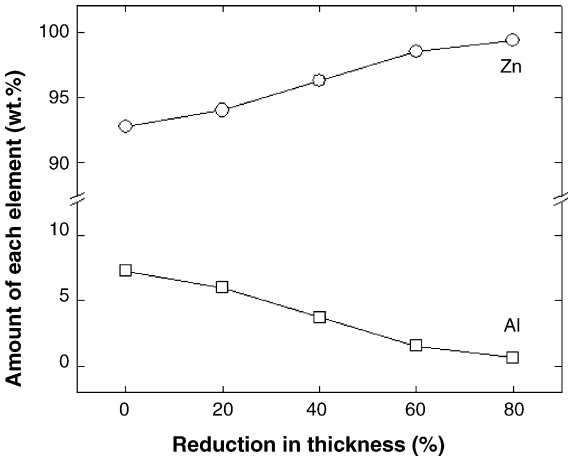

Fig. 10. Changes in Zn and Al contents inside primary η grains with reduction in thickness for Zn–15% Al alloy.

(ii) *Increase in interface area between equiaxed grains possessing high mobility*. Zn–Al alloys are well known for their high intrinsic mechanical damping and room temperature superplasticity due to the boundaries with high mobility [7,8]. Recently, Kurosawa et al. [9] have reported that the mobility of interfaces between equiaxed η and α grains is much greater than that concerning lamellar morphology. It implies that higher volume fraction of η and α grains having equiaxed morphology would lead to yielding at lower stress in response to increase in interfaces with higher mobility. This is well supported by Fig. 9, in which an almost linear relationship between yield strength and volume fraction of equiaxed η and α grains is established.

(iii) *Precipitation of dissolved Al solutes from primary η grains*. Fig. 10 represents the compositional changes of Zn and Al inside primary η grains with reduction in thickness for the Zn–15% Al alloy. Even though the precipitation of dissolved Al from primary η grains during cold rolling was not directly observed in the microstructures given in Figs. 4–7, Fig. 10 clearly shows the increase in Zn content accompanied by decrease in Al content inside primary η grains with the increase in cold rolling, confirming the precipitation of dissolved Al during cold rolling. Considering the difference in atomic radius between Zn (0.133 nm) and Al (0.143 nm), the precipitation of Al solute atoms from η grains would deteriorate the solution hardening effect.

4. Summary

Fully annealed microstructure of the Zn–15% Al alloy consists of primary η grains and (η + α) lamellar colonies. The hardness and yield strength become lower with increasing cold rolling degree, showing work softening. During cold rolling, (η + α) lamellar colonies gradually change into equiaxed η and α grains due to dynamic recrystallization. The compositional analyses on primary η grains by EDS reveal that cold rolling causes precipitation of dissolved Al solutes from primary η grains. In view of these results, change of (η + α) phases from fine lamellar to equiaxed morphology, which gives rise to structural softness along with increase in equiaxed η/α phase boundaries with higher mobility, and deterioration of solution hardening effect by precipitation of dissolved Al from primary η grains, are thought to be responsible for the work softening behavior of Zn–15% Al alloy.

References

[1] M. Knepper, J. Spriestersbach, Proceedings of the ITSC Shanghai 1997, Beijing, November 18–21, 1997, p. 384.
[2] S. Yamamoto, T. Uda, J. Imahori, J. Japan Inst. Met. 3 (1996) 254.
[3] S. Yamamoto, T. Sakaguchi, T. Uda, J. Japan Inst. Met. 3 (1996) 247.
[4] Y.H. Zue, H.C. Man, W.B. Lee, Mater. Sci. Eng. A 268 (1999) 147.
[5] E.O. Hall, Proc. Phys. Soc. B 64 (1951) 747.
[6] N.J. Petch, J. Iron Steel Inst. 174 (1953) 25.
[7] Z. Ma, F. Han, J. Wei, J. Gao, Metall. Mater. Trans. 32A (2001) 2657.
[8] P. Shariat, R.B. Vastava, T.G. Langdon, Acta Metall. 30 (1982) 285.
[9] T. Kurosawa, T. Otani, K. Hoshino, J. Phys. IV 6 (1996) C8–309.